# Supporting Information

## Customizing Pore System in a Microporous Metal-Organic Framework for Efficient $C_2H_2$ Separation from $CO_2$ and $C_2H_4$

Qiang Zhang†, Guan-Nan Han†, Xin Lian, Shan-QingYang, Tong-Liang Hu*

School of Materials Science and Engineering, National Institute for Advanced Materials, Nankai University, Tianjin 300350, China.

* Correspondence: tlhu@nankai.edu.cn (T.-L. Hu)

† These authors contributed equally to this work.

**Table S1**. Crystal data and structure refinement parameters for **NUM-14**

| | |
|---|---|
| Empirical formula | $C_{26}H_{17}N_7NiO_7$ |
| Formula weight (g $mol^{-1}$) | 607.82 |
| Crystal system | trigonal |
| *Space group* | $P3_121$ |
| a (Å) | 15.11740(1) |
| b (Å) | 15.11740(1) |
| c (Å) | 18.8520(2) |
| α(°) | 90 |
| β(°) | 90 |
| γ(°) | 120 |
| V ($Å^3$) | 3731.14(6) |
| Z | 3 |
| $\rho_{calc}$ (g $cm^{-3}$) | 0.812 |
| μ ($mm^{-1}$) | 0.849 |
| F (000) | 933.0 |
| 2Θ range for data collection/° | 6.752 to 147.228 |
| Index ranges | $-18 \leq h \leq 15$, $-13 \leq k \leq 18$, $-23 \leq l \leq 17$ |
| Reflections collected | 12400 |
| Independent reflections | 4868 [$R_{int}$ = 0.0206, $R_{sigma}$ = 0.0236] |
| Goodness-of-fit on $F^2$ | 1.075 |
| Final R indexes [I>=2σ (I)][a] | $R_1$ = 0.0339, $wR_2$ = 0.0967 |
| Final R indexes [all data][b] | $R_1$ = 0.0354, $wR_2$ = 0.0991 |
| Largest diff. peak/hole/e $Å^{-3}$ | 0.21/-0.21 |
| CCDC deposition number | 2163045 |

[a] $R_1 = \sum || F_o | - |F_c|| / \sum |F_o|$, [b] $wR_2 = \{\sum [w(F_o^2 - F_c^2)^2] / \sum w(F_o^2)^2\}^{1/2}$

**Table S2.** Comparisons of $C_2H_2$ uptake and selectivities of $C_2H_2/CO_2$ and $C_2H_2/C_2H_4$ for **NUM-14a** and other MOFs

| **MOFs** | **$C_2H_2$ uptake mmol $g^{-1}$** | **$C_2H_2/CO_2$ (50:50, v/v) selectivity** | **Ref.** |
|---|---|---|---|
| CuI@UiO-66-$(COOH)_2$ | 2.14 | 185.00 | [1] |
| ATC-Cu | 5.01 | 53.60 | [2] |
| MOF-OH | 3.04 | 25.00 | [3] |
| IPM-101 | 3.04 | 12.3 | [4] |
| FJU-118a | 3.96 | 7.80 | [5] |
| BUT-85 | 2.95 | 6.10 | [6] |
| $[Ca(dtztp)_{0.5}]$ | 4.91 | 1.70 | [7] |
| $[Ni(tzba)_{0.5}(F)(bpy)]$ | 5.58 | 2.20 | [8] |
| CAU-10H | 5.13 | 2.50 | [9] |
| SNNU-5-Sc | 5.13 | 2.66 | [10] |
| **NUM-14a** | 4.44 | 3.37 | **This work** |
| **MOFs** | **$C_2H_2$ uptake mmol $g^{-1}$** | **$C_2H_2/C_2H_4$ (1:99, v/v) selectivity** | **Ref.** |
| NUM-12a | 4.42 | 1.13 | [11] |
| Zn(ad)(int) | - | 1.61 | [12] |
| ZJNU-14 | 4.00 | 1.59 | [13] |
| ZJNU-7 | 5.04 | 1.77 | [14] |
| UiO-67-$(NH_2)_2$ | 5.90 | 2.1 | [15] |
| **NUM-14a** | 4.44 | 1.63 | **This work** |

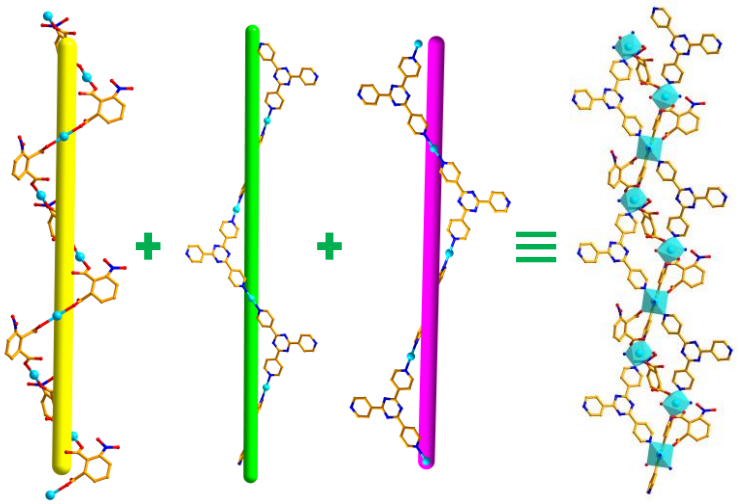

**Figure S1**. Three kinds of helix chains constitute the channel column of **NUM-14**.

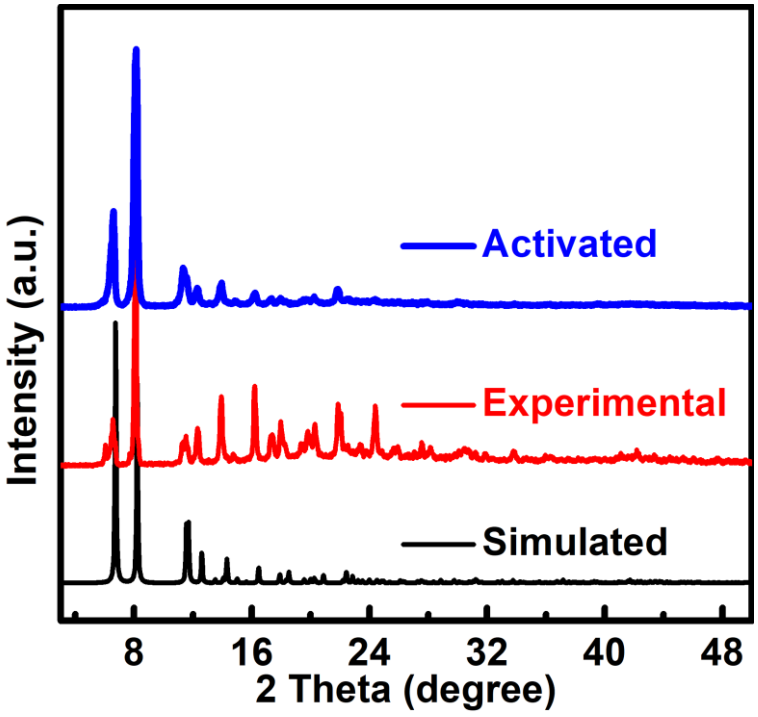


**Figure S2**. Comparison of simulated, experimental, and activated PXRD patterns of **NUM-14**.

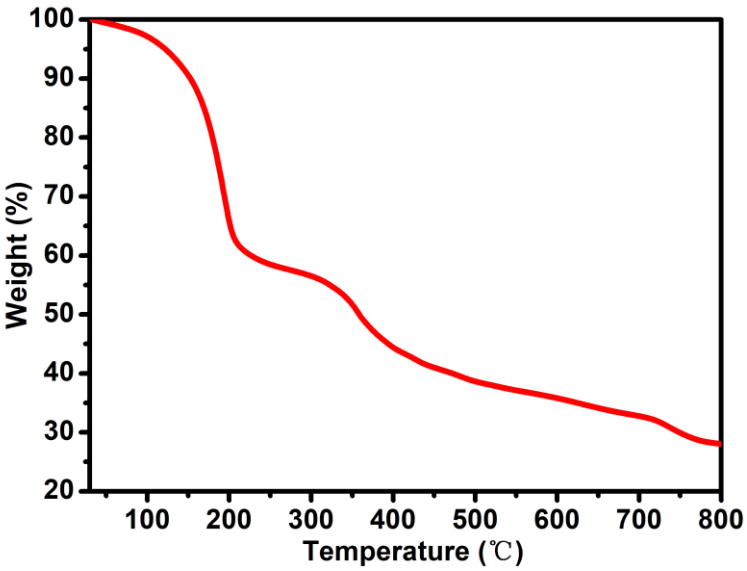


**Figure S3**. TGA curve for **NUM-14** under Ar atmosphere.

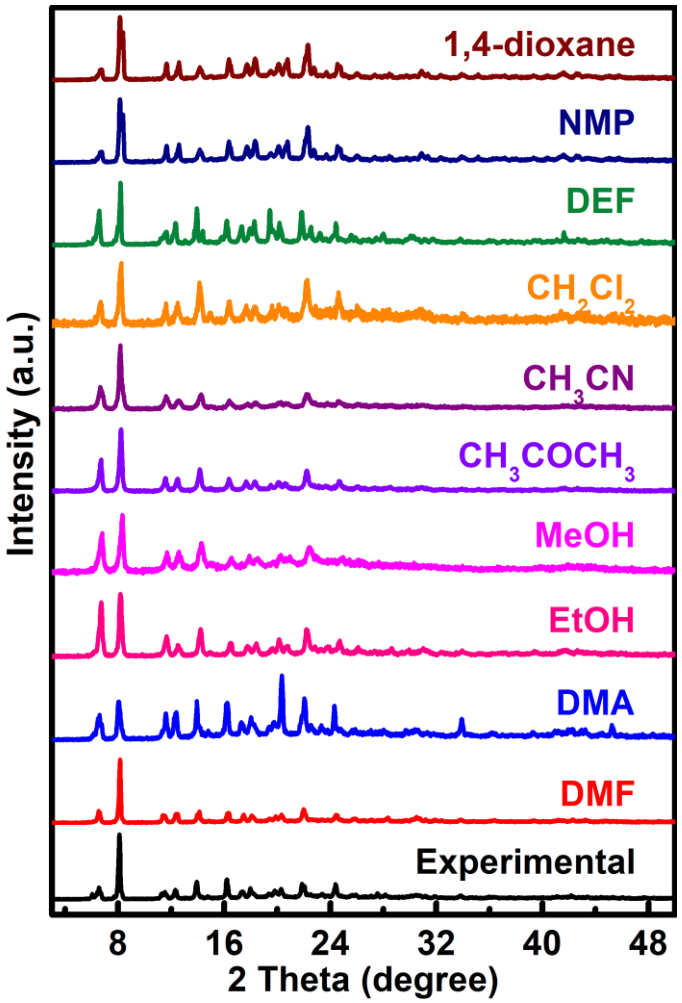


**Figure S4**. The PXRD patterns for **NUM-14** after immersed in common solvents a week.

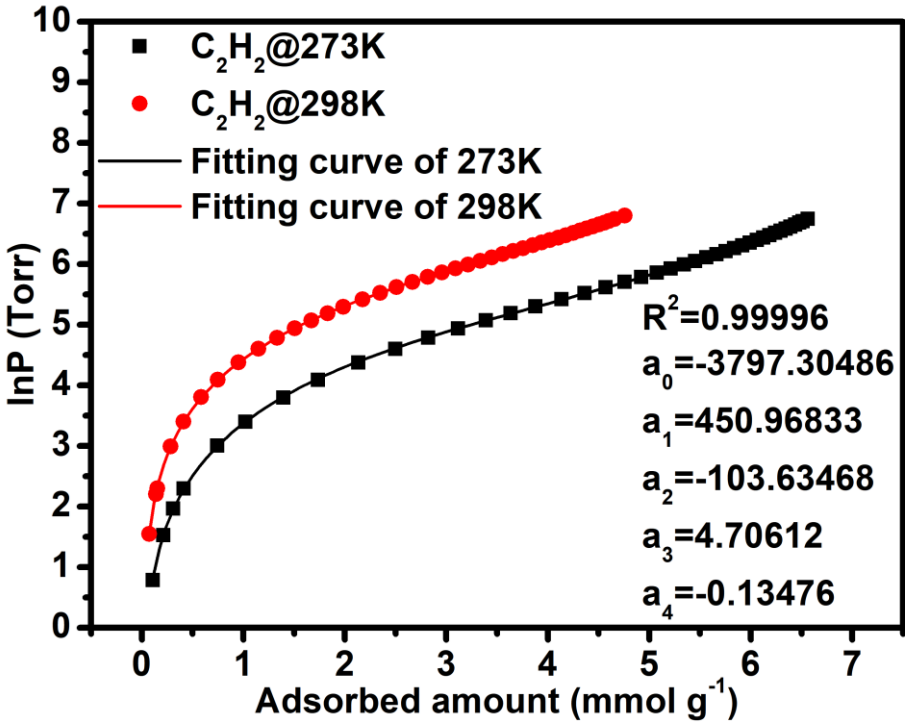


**Figure S5**. The details of Virial equation (solid lines) fitting to the experimental $C_2H_2$ adsorption data (symbols) for **NUM-14a**.

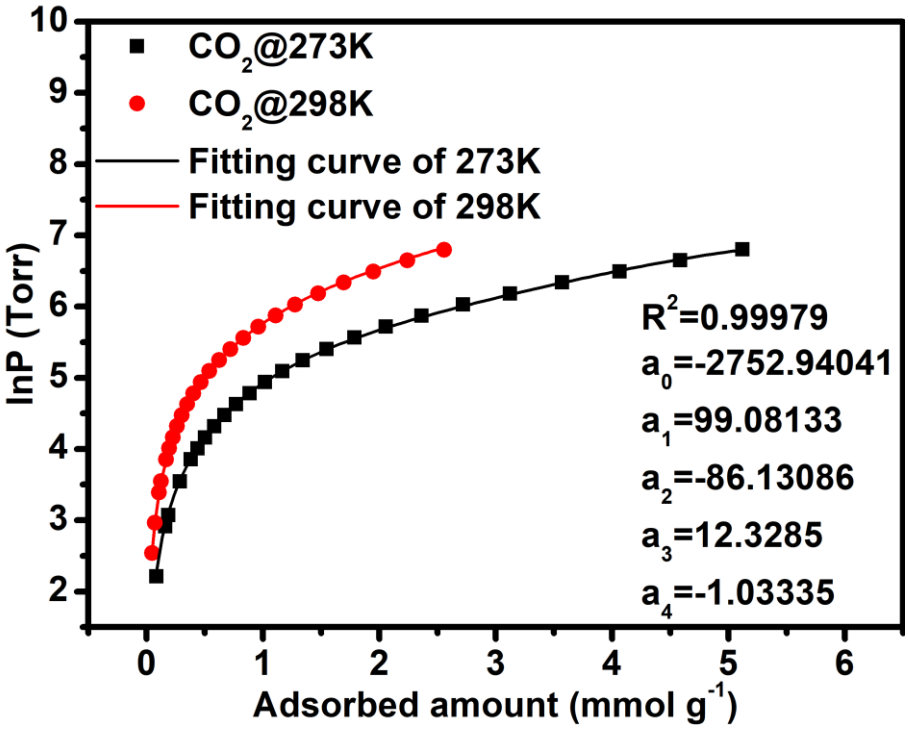


**Figure S6**. The details of Virial equation (solid lines) fitting to the experimental $CO_2$ adsorption data (symbols) for **NUM-14a**.

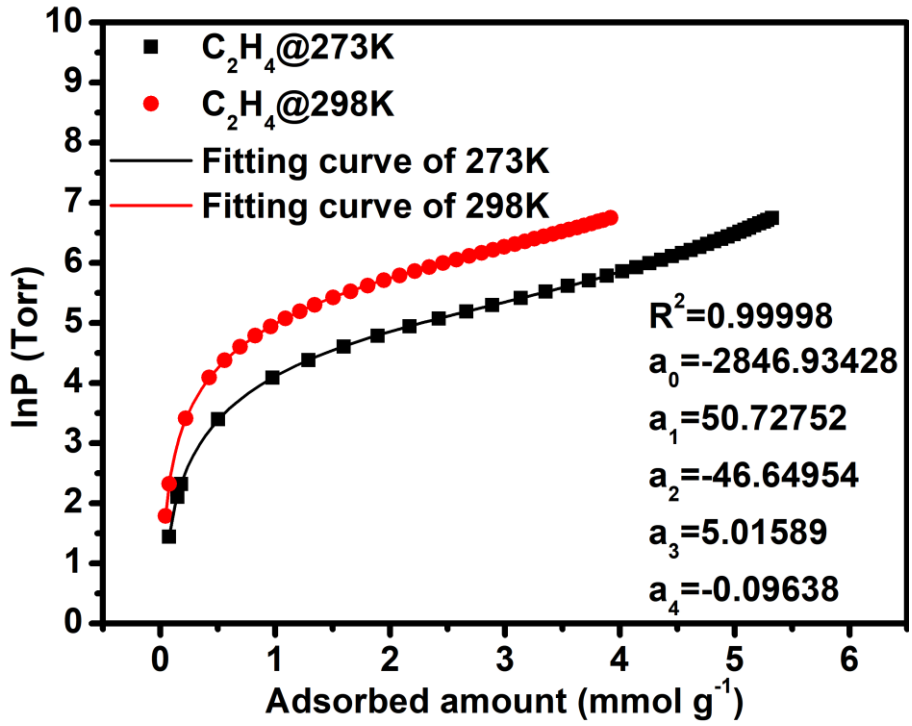


**Figure S7**. The details of Virial equation (solid lines) fitting to the experimental $C_2H_4$ adsorption data (symbols) for **NUM-14a**.

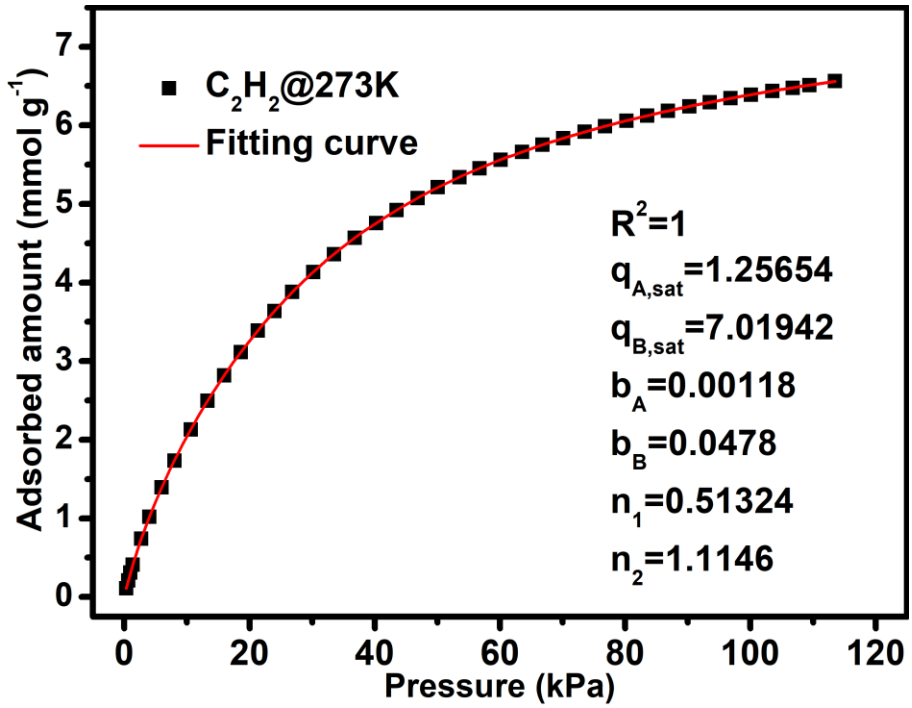


**Figure S8**. The details of dual-site Langmuir-Freundlich isotherm (solid lines) fitting to the experimental $C_2H_2$ adsorption data (symbols) for **NUM-14a** at 273 K.

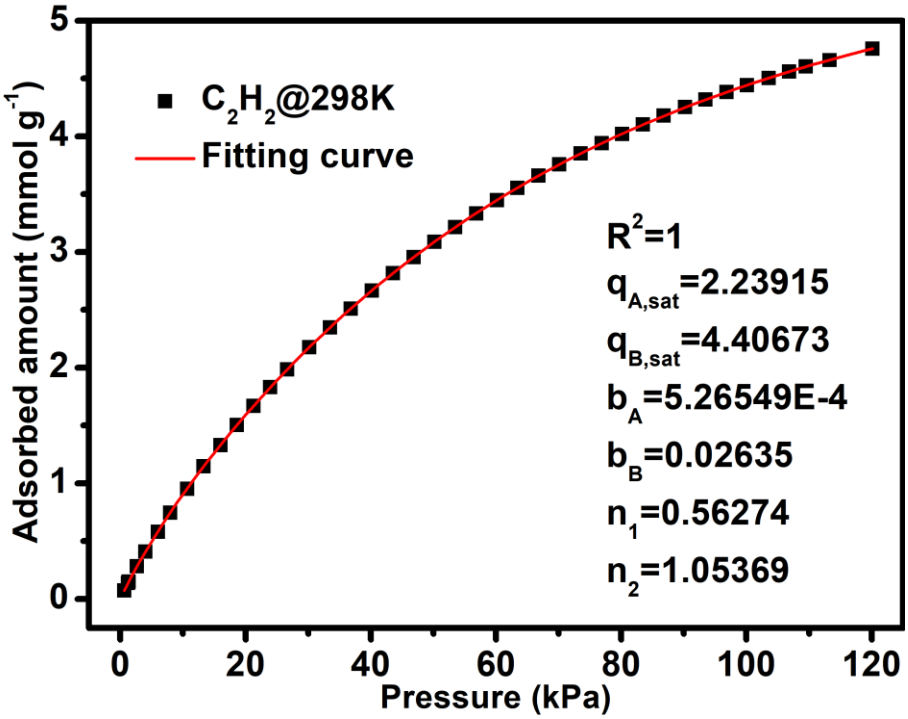


**Figure S9**. The details of dual-site Langmuir-Freundlich isotherm (solid lines) fitting to the experimental $C_2H_2$ adsorption data (symbols) for **NUM-14a** at 298 K.

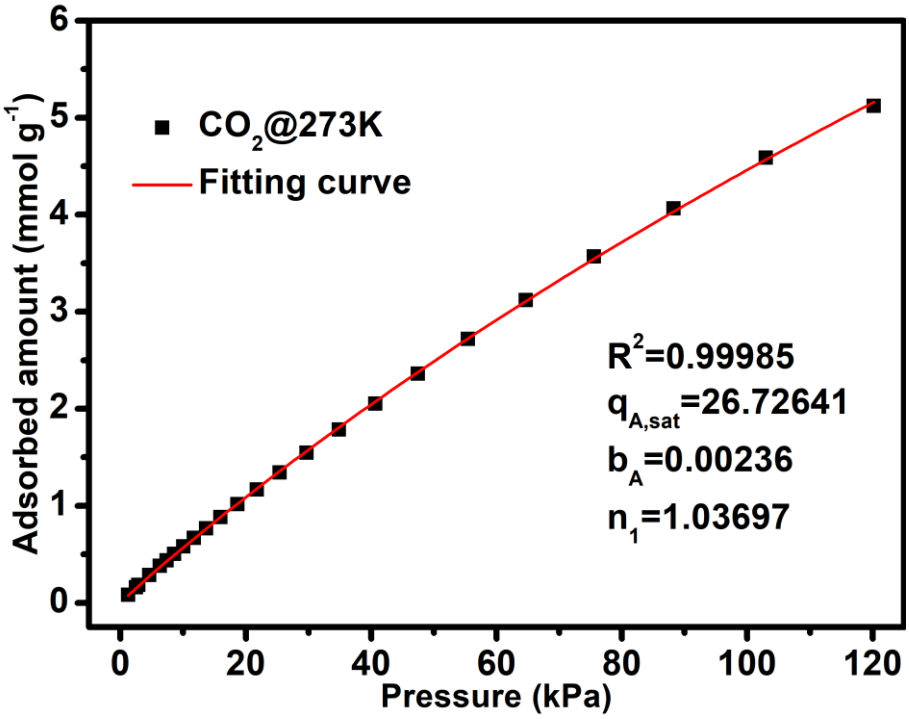


**Figure S10**. The details of single-site Langmuir-Freundlich isotherm (solid lines) fitting to the experimental $CO_2$ adsorption data (symbols) for **NUM-14a** at 273 K.

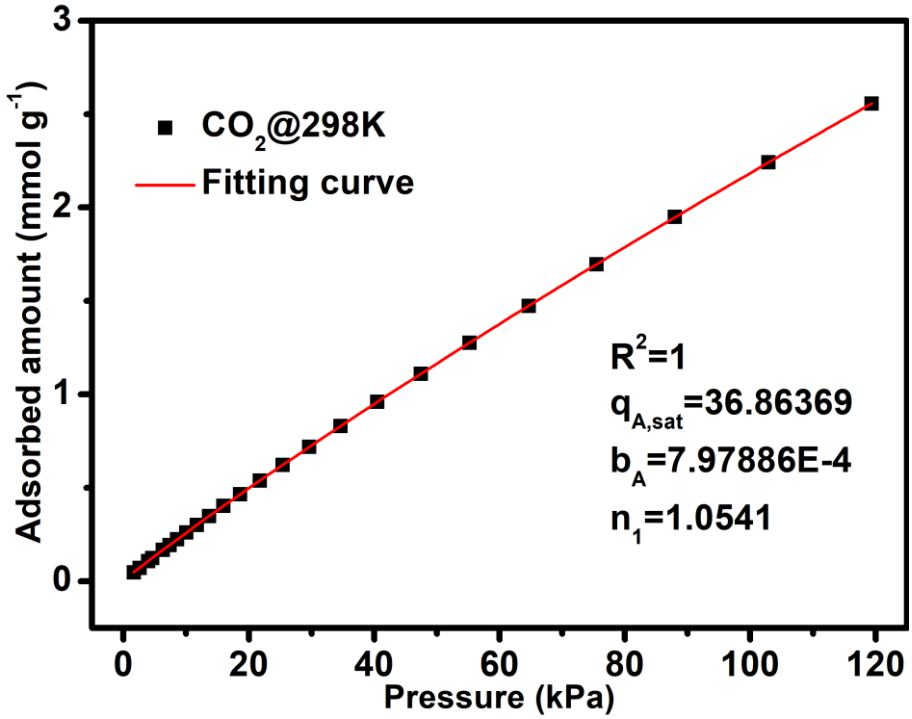


**Figure S11**. The details of single-site Langmuir-Freundlich isotherm (solid lines) fitting to the experimental $CO_2$ adsorption data (symbols) for **NUM-14a** at 298 K.

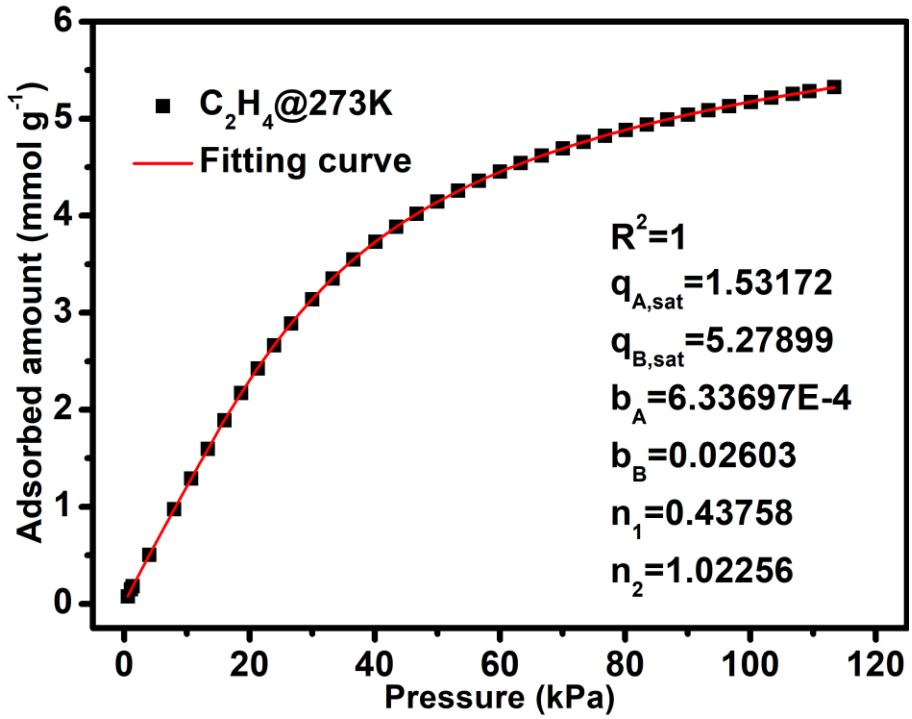


**Figure S12**. The details of dual-site Langmuir-Freundlich isotherm (solid lines) fitting to the experimental $C_2H_4$ adsorption data (symbols) for **NUM-14a** at 273 K.

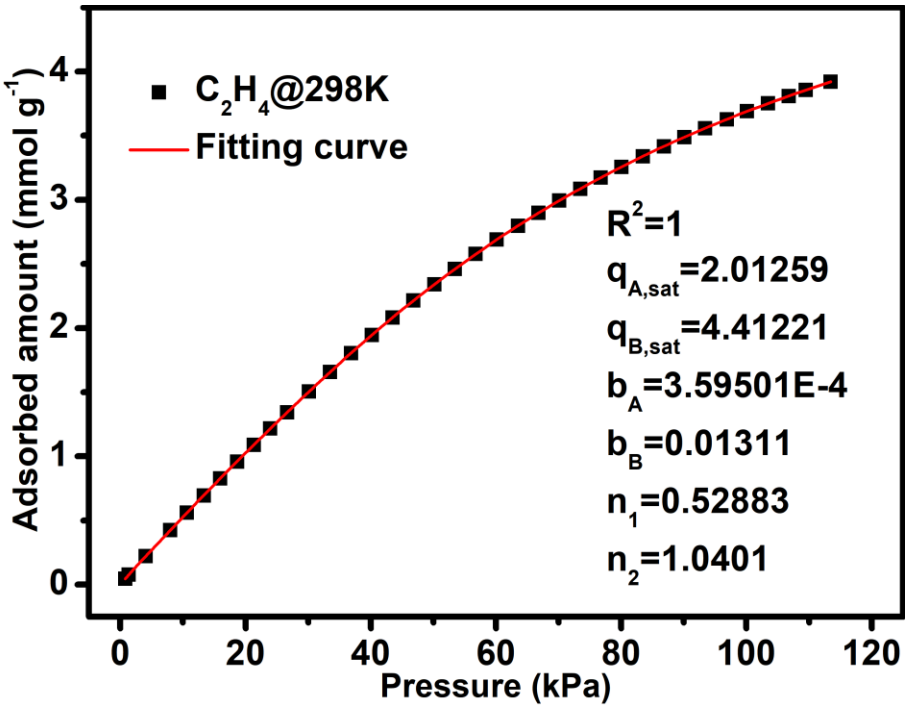


**Figure S13**. The details of dual-site Langmuir-Freundlich isotherm (solid lines) fitting to the experimental $C_2H_4$ adsorption data (symbols) for **NUM-14a** at 298 K.

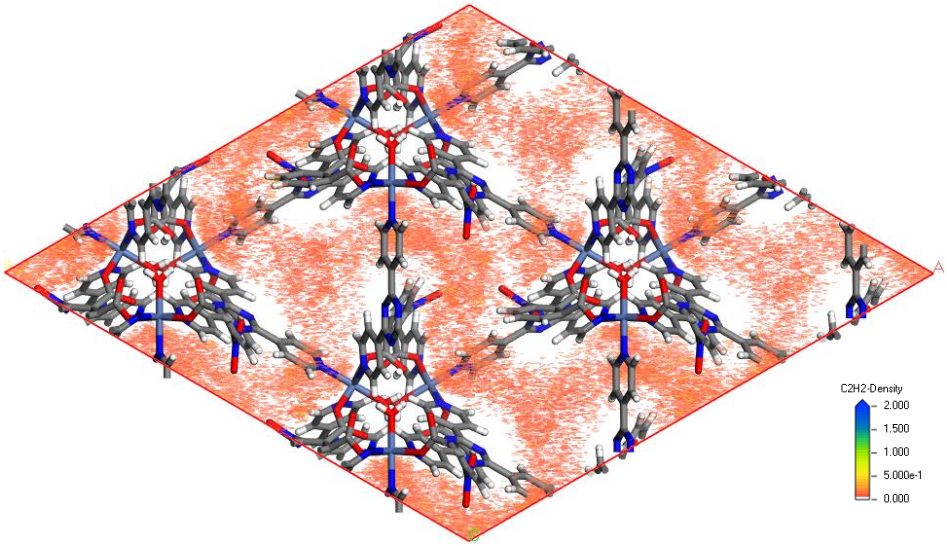


**Figure S14.** Density distribution of $C_2H_2$ in **NUM-14a** at 298 K and 1 bar.

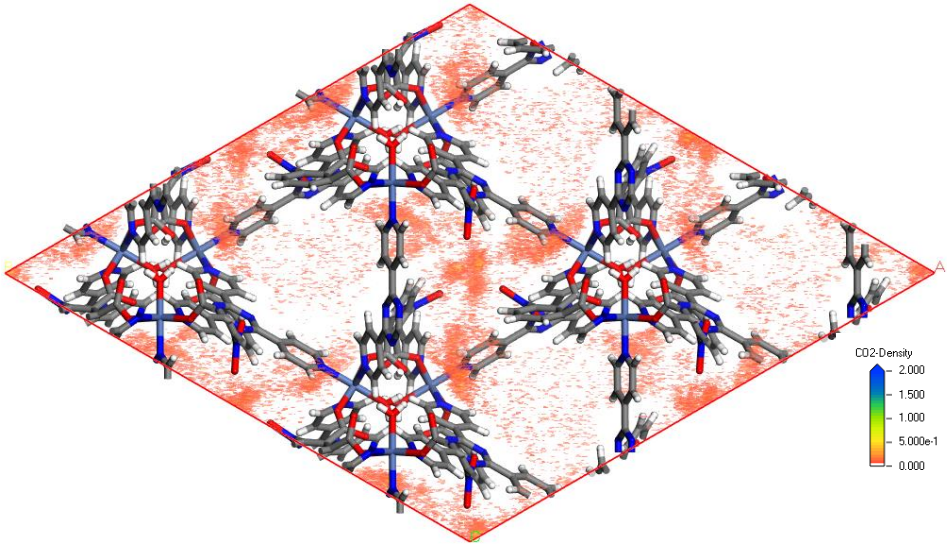


**Figure S15.** Density distribution of $CO_2$ in **NUM-14a** at 298 K and 1 bar.

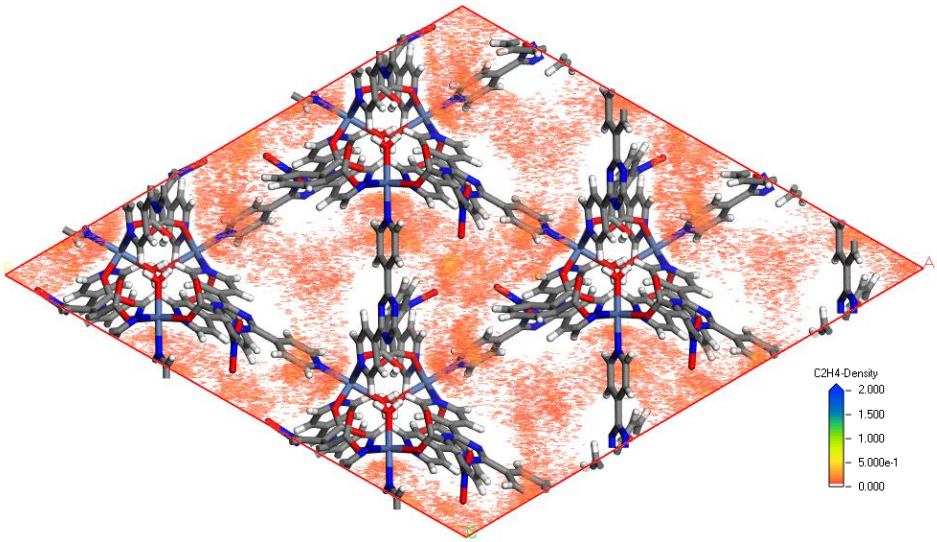


**Figure S16.** Density distribution of $C_2H_4$ in **NUM-14a** at 298 K and 1 bar.

## References


1. Zhang, L.; Jiang, K.; Yang, L.; Li, L.; Hu, E.; Yang, L.; Shao, K.; Xing, H.; Cui, Y.; Yang, Y.; Li, B.; Chen, B.; Qian, G. Benchmark $C_2H_2/CO_2$ separation in an ultra-microporous metal-organic framework via copper(I)-alkynyl chemistry. *Angew. Chem. Int. Ed.* **2021,** *60, 15995-16002.*

2. Niu, Z.; Cui, X.; Pham, T.; Verma, G.; Lan, P. C.; Shan, C.; Xing, H.; Forrest, K. A.; Suepaul, S.; Space, B.; Nafady, A.; Al-Enizi, A. M.; Ma, S., A MOF-based ultra-strong acetylene nano-trap for highly efficient $C_2H_2/CO_2$ separation. *Angew. Chem. Int. Ed.* **2021**, *60, 5283-5288.*

3. Gong, W.; Cui, H.; Xie, Y.; Li, Y.; Tang, X.; Liu, Y.; Cui, Y.; Chen, B., Efficient $C_2H_2/CO_2$ separation in ultramicroporous metal-organic frameworks with record $C_2H_2$ storage density. *J. Am. Chem. Soc.* **2021**, *143, 14869-14876.*

4. Sharma, S.; Mukherjee, S.; Desai, A. V.; Vandichel, M.; Dam, G. K.; Jadhav, A.; Kociok-Köhn, G.; Zaworotko, M. J.; Ghosh, S. K., Efficient capture of trace acetylene by an ultramicroporous metal-organic framework with purine binding sites. *Chem. Mater. 2021,* **33**, *5800-5808.*

5. Song, Q.; Yang, Y.; Yuan, F.; Zhu, S.; Wang, J.; Xiang, S.; Zhang, Z., Electrostatic force-driven lattice water bridging to stabilize a partially charged indium MOF for efficient separation of $C_2H_2/CO_2$ mixtures. *J. Mater. Chem. A* **2022**, *10, 9363-9369.*

6. Si, G.-R.; Wu, W.; He, T.; Xu, Z.-C.; Wang, K.; Li, J.-R., Stable Bimetallic Metal-organic framework with dual-functional pyrazolate-carboxylate ligand: Rational construction and $C_2H_2/CO_2$ separation. *ACS Materials Letters* **2022**, *4, 1032-1036.*

7. Wang, G.-D.; Li, Y.-Z.; Zhang, W.-F.; Hou, L.; Wang, Y.-Y.; Zhu, Z., Acetylene separation by a Ca-MOF containing accessible sites of open metal centers and organic groups. *ACS Appl. Mater. Interfaces* **2021**, *13, 58862-58870.*

8. Wang, G.-D.; Wang, H.-H.; Shi, W.-J.; Hou, L.; Wang, Y.-Y.; Zhu, Z., A highly stable MOF with F and N accessible sites for efficient capture and separation of acetylene from ternary mixtures. *J. Mater. Chem. A* **2021**, *9, 24495-24502.*

9. Ye, Y.; Xian, S.; Cui, H.; Tan, K.; Gong, L.; Liang, B.; Pham, T.; Pandey, H.; Krishna, R.; Lan, P. C.; Forrest, K. A.; Space, B.; Thonhauser, T.; Li, J.; Ma, S., Metal-organic framework based hydrogen-bonding nanotrap for efficient acetylene storage and separation. *J. Am. Chem. Soc.* **2022**, *144, 1681-1689.*

10. Lv, H.-J.; Zhang, J.-W.; Jiang, Y.-C.; Li, S.-N.; Hu, M.-C.; Zhai, Q.-G., Micropore regulation in ultrastable $[Sc3O]^-$ organic frameworks for acetylene storage and purification. *Inorg. Chem.* **2022**, *61, 3553-3562.*

11. Zhang, Q.; Yang, S.-Q.; Zhou, L.; Yu, L.; Li, Z.-F.; Zhai, Y.-j.; Hu, T.-L., Pore-space partition through an embedding metal-carboxylate chain-induced topology upgrade strategy for the separation of acetylene/ethylene. *Inorg. Chem.* **2021**, *60, 19328-19335.*

12. Ding, Q.; Zhang, Z.; Liu, Y.; Chai, K.; Krishna, R.; Zhang, S. One-step ethylene purification from ternary mixtures in a metal-organic framework with customized pore chemistry and shape. *Angew. Chem. Int. Ed.* **2022**, *DOI: 10.1002/anie.202208134.*

13. Jiang, Z.; Fan, L.; Zhou, P.; Xu, T.; Chen, J.; Hu, S.; Chen, D.-L.; He, Y., An N-oxide-functionalized nanocage-based copper-tricarboxylate framework for the selective capture of $C_2H_2$. *Dalton Transactions* **2020**, *49, 15672-15681.*

14. Jiang, Z.; Fan, L.; Zhou, P.; Xu, T.; Hu, S.; Chen, J.; Chen, D.-L.; He, Y., An aromatic-rich cage-based MOF with inorganic chloride ions decorating the pore surface displaying the preferential adsorption of $C_2H_2$ and $C_2H_6$ over $C_2H_4$. *Inorg. Chem. Front.* **2021**, *8, 1243-1252.*

*15.* Gu, X.-W.; Wang, J.-X.; Wu, E.; Wu, H.; Zhou, W.; Qian, G.; Chen, B.; Li, B., Immobilization of lewis basic sites into a stable ethane-selective MOF enabling one-step separation of ethylene from a ternary mixture. *J. Am. Chem. Soc.* **2022**, *144, 2614-2623.*